# Resonant Waveguide vs Fabry-Perot Cavity: A Comparative Study for CMOS Spectral Sensor Technology

Fatima Omeis,[1] Sandrine Villenave, [1,2,3] Mondher Besbes,[1] Christophe Sauvan,[1] and Henri Benisty[1]

[1] Laboratoire Charles Fabry, Institut d'Optique Graduate School, Université Paris Saclay, CNRS, Palaiseau, France
[2] STMicroelectronics, 38920, Crolles, France
[3]Univertsité Grenoble Alpes, CEA Leti, Grenoble, France

*In recent years, the huge increase in the use of versatile smart devices spurred a rapid growth in spectral sensor technology. Nowadays, the majority of these devices rely on the use of complementary metal-oxide semiconductor (CMOS) technology, especially for Ambient Light Sensors (ALS) applications. In this study, we provide a performance comparison study between two candidate filtering structures, the resonant waveguide (RWG) and the Fabry Perot (FP) cavity. The evaluation is carried out in terms of spectral response, angular and polarization tolerance, tunability, noise sensitivity, and light collection. Through this analysis, guidance is provided for engineers in terms of application choice and sensing capability.*

## Introduction

In the last decades, the technology sector and the microelectronics industry are experiencing rapid market progressions. Thanks to miniaturization driving the ubiquitous use of smartphones and cameras in all environments, this has led to an explosion of the demand for integrated spectral sensors with various functions. Among these, ambient light sensors (ALS), especially for operation in the infrared range, are of interest in smart phone cameras, color correction, screen-brightness adjustment and surveillance and monitoring systems [1]. The underlying filters rest on the interaction of light with subwavelength structures (dielectric or metallic). Their fabrication process relies on the mature complementary metal oxide semiconductor (CMOS) techniques offering scalability for mass production.

In this study we will provide a guide for ALS filter choice by exploring, comparing, and evaluating the performance of two potential designs for spectral filters in the near infrared range, the resonant waveguide (RWG) and the Fabry-Perot (FP) cavity designs [2][3]. The spectral response of both structures will be studied and compared, while their scalability, in wavelength terms here, and their tunability are tested, taking into account parsimony in the fabrication process steps. Moreover, the angular tolerance for both TE and TM polarization is discussed. Finally, a preliminary comparative study on the signal-to-noise performance in terms of coarse spectral retrieval on both types of configurations is reported, based on the useful case of chlorophyll (plant leaves) diffuse reflection.

## 1- Structures' design, spectral response, and tunability

The structures detailed in Fig.1 comprise few layers and a simple shape (a square "atom") easily controlled in a CMOS process on a fairly large range of its filling factor *f*. The first comparison in this study is the spectral response of both structures when illuminated with linearly polarized wave. The RWG filter is represented schematically in Fig1.(a) it

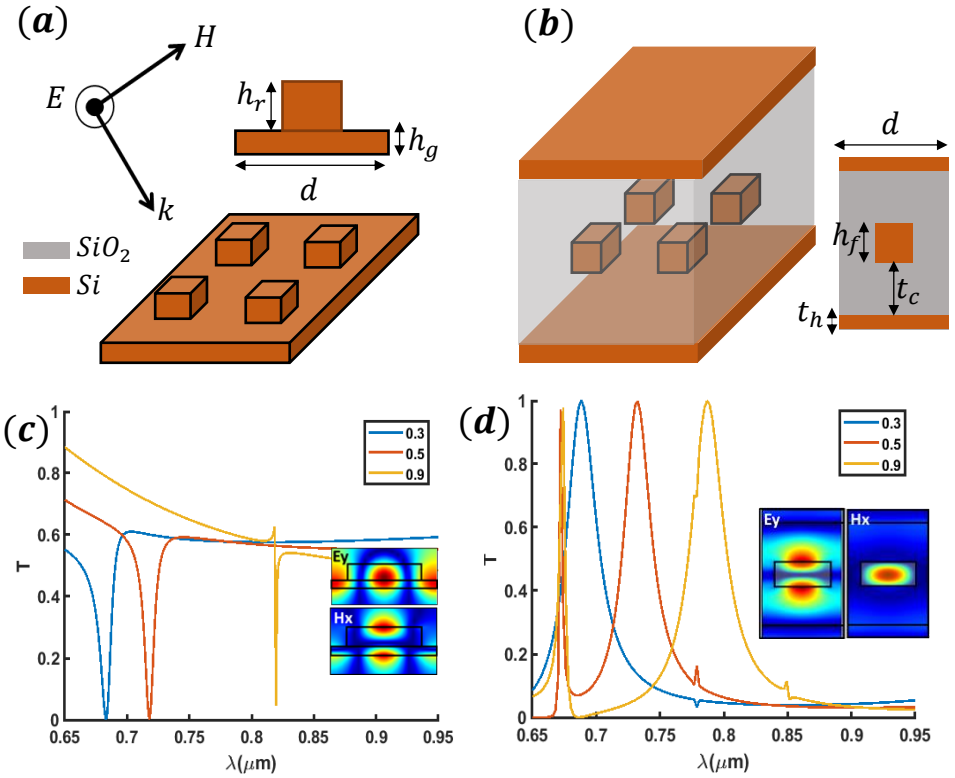


Figure 1: (a-b) Sketch of RWG structure of period d, thickness of the grating $h_r$=50 nm and $h_g$=25 nm for the waveguide and of the FP filter (d=300 nm, $h_f$=100 nm, $t_c$=150 nm, $t_h$=50 nm); brown is *a*-Si, the rest is $SiO_2$ . (c-d) Transmission spectra for the three indicated filling factors *f* . See text for field map insets.

consists of a thin layer ($h_g$ = 25 nm) of refractive index $n_{Si}$ = 4, which is an approximation of that of *a*-Si in the spectral range studied, and a square *a*-Si grating of thickness $h_r$ = 50 nm. On the other hand, the FP filter, shown in Fig.1(b), is composed of a square grating of thickness $h_f$ = 100 nm (a metamaterial), embedded between two thin Si layers ($t_h$ = 50 nm) and spaced by silica ($SiO_2$, $n_{SiO2}$=1.456, $t_c$ = 150 nm). For the RWG, when a TE polarized plane wave irradiates the structure at θ = 0° and φ = 0°, a narrow transmission dip (hence a reflection peak) is generated, Fig.1(c). This is due to the grating coupling the incident wave to a structure's leaky waveguide mode ($k=n_{eff}\ 2\pi/\lambda$) [4]. Upon increasing *f* in the indicated feasible range, it is clearly seen that the reflection peak is redshifted by ~ 150 nm. This is due to the increase of $n_{eff}$ via the increased grating average index. It is worth noting that the dip width decreases for large *f* (which can skew the spectral performance). On the other hand, the FP filter (also made of solely *a*-Si and $SiO_2$) produces transmission peaks up to 100%, on account of well-known multiple interferences and energy storage inside the mirrors [5]. This peak varies in a similar redshifted way as the RWG filter with *f*, Fig.1 (d), the basic reason being the sole average index. While the RWG dip was thinned for large *f*, the transmission peak in the FP filter *retains its shape, width, and its high transmission efficiency.* We have tested various feasible shapes and lattices and reached in all cases similar conclusions: only the FP approach can produce a set of filters mimicking a spectrometer's job (i.e., well-shaped similar channels gently covering the IR range), not the RWG. But in a system's perspective, those aspects of RWG at odds with a basic spectrometer picture could be mitigated by signal processing taking into account its special response.

## 2-Electric and magnetic field distribution for RWG and FP filters

In order to visualize the resonant modes in each kind of filter and grasp which features are critical, the electric and magnetic field distributions are calculated for TE polarization and at normal incidence($\theta = 0$). The geometrical parameters of the RWG and the FP filters are chosen as mentioned before, with $f$ = 0.5. For the RWG case, the resonance is found at $\lambda_{RWG}$ = 718 nm. The insets of Fig.1(c) show respectively the y-component of the E field, and the x-component of H field in the (xz-plane) which obey the expected pattern for a guided mode with wavevector k along x. For the FP case now, still with $f$ = 0.5, the resonance is at $\lambda_{FP}$ = 717 nm. As shown in Fig.1 (d) insets, the electric field pattern is concentrated on the top and bottom faces of the silicon atom, which points to the 2nd order FP mode. The magnetic field is concentrated inside the silicon atom. The electric field is weak at both mirrors due to the overall π phase reflection of the thin slabs.

## 3-Polarization and angular tolerance

Another criterion, worth investigating for several of the above applications, is to assess the angular tolerance of RWG vs FP under oblique incidence. Fig. 2 shows their transmission map [i.e. maps of T($k_{//}$,ω) with $k_{//} = \sin\theta\,(2\pi/\lambda)$ that we nickname dispersion maps given their salient features] in TE and TM polarization for $\phi$=0°. Fig.2(a) concerns TE polarization for RWG. It appears that the RWG structure is very sensitive to θ or $k_{//}$, indeed the predicted behavior for a canonical grating waveguide ($k_{//}+2\pi/d=n_{eff}\,[2\pi/\lambda]$ at constant $n_{eff}$). The resonant wavelength is shifted from ($d/\lambda$) = 0.415 to 0.465 at ~20°. Remarkably, for TM now, the resonant dip remains quite unaffected until θ ≳20°. We will discuss which coupling specific of 2D grating is involved in this attractive feature. As for the FP filter, either in TE or TM cases, it has little dispersion (less than a canonical FP [3]). Specifically, the dispersion for TE still follows a nanostructured FP blueshift trend, but not in TM where dispersion nearly vanishes due to deep and complex modal interactions. From this comparison, one can deduce that the FP structure provides a larger angular tolerance compared to the RWG, unless only TM is targeted.

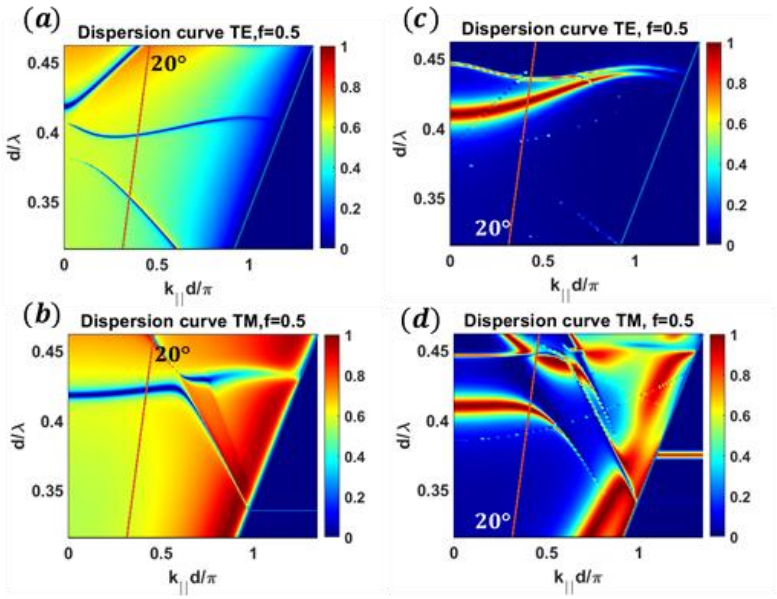


Figure 2: (a-b) respectively represent the dispersion map T ($k_{//}$,ω) of the TE and TM polarization for the RWG structure for (f=0.5, $t_g$=25nm, and $t_h$=50nm). (c-d) correspond respectively to the dispersion map of the TE and TM polarization for the FP structure for (f=0.5, d=300, $h_f$=100, $t_c$=150, $t_h$=50nm).

## 4- Signal to noise ratio (SNR) and light collection

A reasonable "ALS target" is to retrieve a coarse spectrum from a set of $N$~10 ALS sensors with stepped $f$ interpolated from the three $f$'s of Fig.1. Without noise, it boils down to an inversion problem with $N$ degrees of freedom. Then, it suffices that the $N\times N$ matrix $M$ relating $N$ "spectral bins" to $N$ ALS sensors has an inverse $M^{-1}$. In the presence of noise, the conditioning of $M$ dictates how valuable the inversion is. Without the noise issue, matrices $M$ for RWG and for FP should work equally well, with provisions for the skewed dip width at larger $f$ (the dip becoming much smaller than the spectral bin targeted). In the presence of noise however (scaling, say, as photocurrent$^{1/2}$), the FP is more advantageous. To substantiate this discussion, we present the retrieval of the elementary leaf-type spectrum Fig.3(a), by RWG and FP filters Fig.3(b-c) respectively, with shades for the noise-induced scatter in the result. It is clear that even with the large photon "spectral intake" of the RWG pixel ($\gtrsim$80% of impinging light), the retrieved leaf signal is blurred with an average noise $\bar{\sigma}_{RWG} = 0.18$. However, for the FP pixel, even though most of the impinging light is rejected ($\gtrsim$80% ) it is more successful in retrieving the leaf signal with an average noise $\bar{\sigma}_{FP} = 0.05 \ll \bar{\sigma}_{RWG}$. This ability of noise tolerance in coarse spectral retrieval is positively factored when considering the oblique incidence which will, at the end, add another advantage to the FP filter.

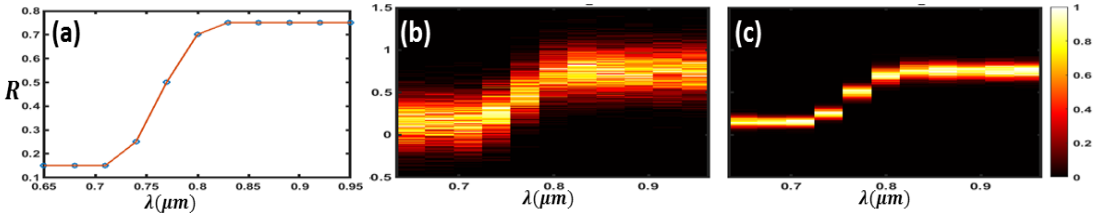


Figure 3: (a) The chlorophyll reflection spectrum from a green leaf. (b) Retrieved spectra from RWG filter. (c) Retrieved spectra from FP filter. Shades show the normalized amount of occurrences in noise-affected retrieval.

## Conclusion

As a conclusion, in this study we provide a summary of the challenging aspects in CMOS sensors to realize near-infrared filtering structures compatible with CMOS technology, as a guidance for technology developers, thus with the capability of building a whole filtering matrix in a single lithographic step. The RWG, that work in rejection mode in the IR range, are a first choice due to their more basic fabrication with a mere silica cover. For FP structures, additional steps on the cover side are needed, but the filters' tolerance vs incident angles is increased. Additionally, signal treatment may be easier and better with transmission filters (cf. Fig.3), all these advantages pointing toward FP filter as an excellent trade-off between process, ease of use, and spectral response of these filters.

## References


[1] S. Dutta, "Point of care sensing and biosensing using ambient light sensor of smartphone: Critical review", TrAC Trends in Analytical Chemistry,110, 393-400, 2019

[2] S.Villenave et al. « Advanced Optical Filtering Based on Si nanodisk Integration on 300mm Glass Wafer." SSDM Conference. 2021

[3] F. Omeis, M. Besbes, C. Sauvan, and H. Benisty, Highly Angular Tolerant Transmission Filters for Narrow-Band Image Sensors. Optics and Photonics Journal, 11, 140-151, 2021

[4] T. Sun, and D. Wu, Guided-mode resonance excitation on multimode planar periodic waveguide, Journal of Applied Physics 108, 063106 (2010)

[5] W. Yue, S. Lee, and E. Kim, "Angle-tolerant polarization-tuned color filter exploiting a nanostructured cavity," Opt. Express 24, 17115-17124 (2016).